Mechanism and Machine Theory 92 (2015) 230–239

Contents lists available at ScienceDirect

Mechanism and Machine Theory

journal homepage: www.elsevier.com/locate/mechmt

Design of a statically balanced fully compliant grasper

A.J. Lamers [a], Juan Andrés Gallego Sánchez [b,*], Just L. Herder [c]

[a] University of Twente, Einschede, The Netherlands
[b] Dept. Mechanical Engineering, Eafit University, Medellin, Colombia
[c] Dept. of Precision and Microsystems Engineering (PME), TUDelft, Delft, The Netherlands

ARTICLE INFO

Article history:
Received 20 February 2015
Received in revised form 15 May 2015
Accepted 25 May 2015
Available online 12 June 2015

Keywords:
Static balancing
Zero stiffness
Pseudo-rigid-body model
Compliant mechanisms
Laparoscopic grasper
Rigid-body-replacement-method

ABSTRACT

Monolithic and thus fully compliant surgical graspers are promising when they provide equal or better force feedback than conventional graspers. In this work for the first time a fully compliant grasper is designed to exhibit zero stiffness and zero operation force. The design problem is addressed by taking a building block approach, in which a pre-existing positive stiffness compliant grasper is compensated by a negative stiffness balancer. The design of the balancer is conceived from a 4-bar linkage and explores the rigid-body-replacement method as a design approach towards static balancing. Design variables and sensitivities are determined through the use of a pseudo-rigid-body model. Final dimensions are obtained using rough hand calculations. Justification of the pseudo rigid body model as well as the set of final dimensions is done by non-linear finite element analysis. Experimental validation is done through a titanium prototype of 40 mm size having an unbalanced positive stiffness of 61.2 N/mm showing that a force reduction of 91.75% is achievable over a range of 0.6 mm, with an approximate hysteresis of 1.32%. The behavior can be tuned from monostable to bistable. The rigid-body-replacement method proved successful in the design of a statically balanced fully compliant mechanism, thus, widening the design possibilities for this kind of mechanism.

1. Introduction

In this article the use of the pseudo-rigid-body-model (PRBM) is shown for the first time in the design of a statically balanced fully compliant grasper. The design and development of a true monolithic prototype are proved valuable in the development of a grasper for minimal invasive surgery. Minimal invasive surgery is a technique in which surgeons access the body cavities by small incision rather than large ones. In this kind of surgery tissue manipulation is carried out by laparoscopic instruments. The instruments besides tissue manipulation, supply the surgeon with sensory feedback. More specific for the grasping instruments, tactile information is provided as force feedback between the input and output of the instrument mechanism. Important design requirements for surgical tools are high force feedback and high sterilizability. Ideally, sterilizability means removing all hinges which are present in conventional tools based on rigid body mechanisms. This can be done by designing a fully compliant grasper. But then elastic stiffness will disturb the force feedback. Statically balanced fully compliant mechanism can cope with these design requirements by providing design possibilities for cheap disposable tools due the monolithic character of fully compliant mechanisms.

In 1997 the urge for high force feedback was recognized and aimed for by designing a rolling contact mechanism replacing the conventional hinged surgical grasper by Herder et al. [1]. In 2000 it was realized by Herder and van den Berg [2] that friction, wearing, and lubrication could be eliminated by moving towards a zero stiffness compliant design, with the added benefits of sterilizability and reduced assembly costs. While a prototype was made, it was not a fully compliant design, it consisted of a 43 N/mm positive stiffness

* Corresponding author.
E-mail addresses: toonlamers@hotmail.com (A.J. Lamers), jgalleg5@eafit.edu.co (J.A. Gallego Sánchez), j.l.herder@tudelft.nl (J.L. Herder).

http://dx.doi.org/10.1016/j.mechmachtheory.2015.05.014
0094-114X/

compliant gripper compensated by a rolling contact mechanism. The balancing mechanism compensates for the elastic forces of the compliant grasper. Later in 2004 Stapel and Herder [3] proposed a feasible solution for a fully compliant version but no prototype was made. De Lange et al. [4] proposed in 2008 a design based on topology optimization, without a proving prototype. In 2009 Tolou and Herder [5] developed a mathematical model for partially compliant bistable segments in order to facilitate the design of a partially compliant balancing mechanism. In 2010 fully compliant balancing segments (negative stiffness building blocks) were introduced by Hoetmer et al. [6]. A prototype was created using these segments but exceeded the yield stress due to the preload force. As known by the authors no successful prototype has been presented yet of a statically balanced fully compliant surgical grasper.

Fully compliant mechanisms are monolithic structures that gain their motion only from the deformation of their constitutive elements — no relative motion between elements due to sliding or rolling kinematic pairs. Compliant mechanisms have benefits such as the absence of sliding friction wear, noise, vibration and the need for lubrication [7]. However, since compliant mechanisms rely on the elastic deflection of its elements, potential energy is stored as strain energy which introduces stiffness affecting the input–output relationship.

The design of compliant mechanisms is based on three main approaches (i) the rigid-body-replacement, (ii) topology optimization [8] and (iii) the building blocks approach [9,10]. In this work we focus on the rigid-body-replacement method [11,12] since it is a straight forward approach, which takes a conventional rigid body mechanism and replaces the overlapping joints by monolithic flexures. The joint replacement procedure makes extensive use of the pseudo-rigid-model (PRBM) which allows finding a rigid-body mechanism with torsion springs that emulates the behavior of a constant cross-section compliant member undergoing large, nonlinear deflections [13].

The rigid-body-replacement method is a rule-based method that allows the designer to keep control over the topology and the stiffness of the flexure joints which is critical if static balancing is to be achieved [14]. Static balancing is a conservative state of motion where the total potential energy is kept constant along the range of motion, which results in a constant static equilibrium of all the internal forces. A mechanism in such a state does not require any force for its actuation besides those to overcome the inertial loads and non-conservative forces such as friction.

Statically balanced compliant mechanisms can be design be reintroducing into the energy stream between input and output, the stored strain energy in the compliant members from another source of elastic potential energy. The latter can be achieved by combining two blocks with opposite or additive inverse stiffness functions [14]. In our case the compliant gripper exhibits a linear stiffness function which is compensated by a balancer with the same negative linear stiffness function.

In the following, the conceptual design and dimensioning of the balancer is presented. Next the validation of the concept is presented by the use of finite elements analysis and the experimental validation of the prototype. In the conclusion chapter assessment of the design criteria and the design approach will be done. The discussion chapter focuses on the recommendations and perspectives of the obtained design as well as the design approach.

2. The grasper

In this work the grasper design presented in [2] is used. This design was manufactured of orthopedic stainless steel and exhibited a linear positive stiffness of 43 N/mm. Such stiffness value will not be considered since in this work the prototype is manufactured of titanium. Dimensions will be kept but the stiffness will be measured in the prototype.

3. The balancer

The balancer has the function of providing a balancing force function with linear negative stiffness opposite to the positive stiffness of the compliant grasper. To simplify the stiffness calculations a building block approach is used. In this approach the desired total force-displacement function (continuous zero force) from the whole system, is decomposed into two additive inverse functions. Here, each function corresponds to each of the building blocks, one block represents the grasper while the other represents the balancer. Since the force-displacement function of each block is designed a priori and independently, when both building blocks are connected, there cannot be unaccounted sources of stiffness. The latter means that the balancer must be connected to the grasper without any relative motion — no kinematic pairs. A way to connect the two building blocks without relative motion between them is through the use of a straight line guidance mechanism. Hence, the balancer is designed from a slider–rocker linkage with torsion springs at its three joints to account for the elastic stiffness of its monolithic version, see Fig. 1.

For this kind of linkage the force-displacement function $F_{Cx} = f(\Delta x_C)$ can be explicitly found at point C. A study is conducted to determine the influence of the design parameters on the stiffness function. The design parameters are set as the link lengths l_1 and l_2, the stiffness k_A, k_B, and k_C of the torsion springs, the pre-loading deflection Δy_A of point A, the initial position $(0, y_A)$, $(x_C, 0)$ of points A and C respectively, and the preloading of the torsion springs θ_2^0, θ_3^0, and φ^0.

The horizontal force at point C for motion under quasi-static condition can be found from the system of equilibrium equations, see Fig. 2. From link 1 reaction f_{B_y} is expressed in terms of reaction f_{B_x}. From link 2 reaction f_{B_x} is solved. Reaction f_{B_x} is equal in magnitude to force F_{C_x} which yields,

$$F_{Cx} = \frac{l_1 \cos\theta_2 (M_B - M_C) - l_2 \cos\theta_3 (M_A + M_B)}{l_1 l_2 \sin(\theta_3 - \theta_2)} \tag{1}$$

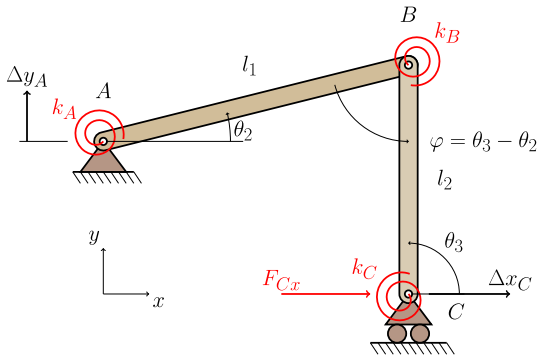

Fig. 1. Slider–rocker linkage model with torsion springs.

where the external moments at the joints correspond to those exerted by the springs and given by,

$$M_A = -k_A\left(\theta_2 - \theta_2^0\right) \tag{2}$$

$$M_B = k_B\left(\theta_3 - \theta_2 - \varphi^0\right) \tag{3}$$

$$M_C = -k_C\left(\theta_3 - \theta_3^0\right). \tag{4}$$

Here, the joint angles θ_2 and θ_3, which are function of the deflection Δx_C, define the configuration of the linkage by,

$$\theta_2 = arccos\left(\frac{l_1^2 - l_2^2 + (y_A + \Delta y_A)^2 + (x_C + \Delta x_C)^2}{2l_1\sqrt{(y_A + \Delta y_A)^2 + (x_C + \Delta x_C)^2}}\right) -$$

$$arctan\left(\frac{y_A + \Delta y_A}{x_C + \Delta x_C}\right) \tag{5}$$

$$\theta_3 = arccos\left(\frac{l_1 cos\,\theta_2 - (x_C + \Delta x_C)}{l_2}\right). \tag{6}$$

The study shows that negative stiffness is promoted when (i) the pre-loading displacement Δy_A at hinge A is in the vertical downward direction (Fig. 3a), (ii) when torsion stiffness on hinge A is larger compared to the stiffness on hinges B an C (see Fig. 3b), and (iii) when the length l_1 is shortened and both links are kept perpendicular to each other at the stress-free configuration (see Fig. 3c). The study reveals that changes on the orientation of l_2 from the vertical at the stress-free configuration shifts the force-deflection behavior. Increasing the length l_2 improves the linearity of the negative stiffness behavior (see Fig. 3d).

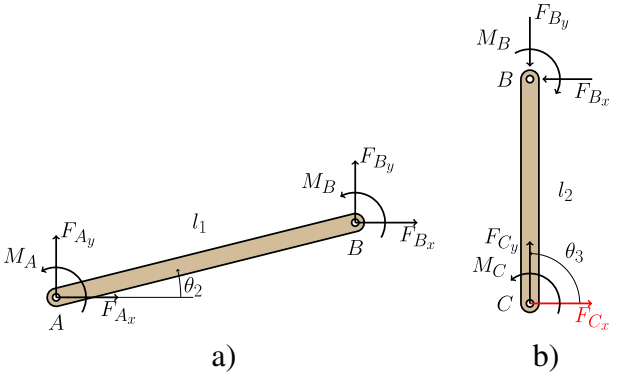

Fig. 2. Free-Body diagram. (a) Link AB. (b) Link BC.

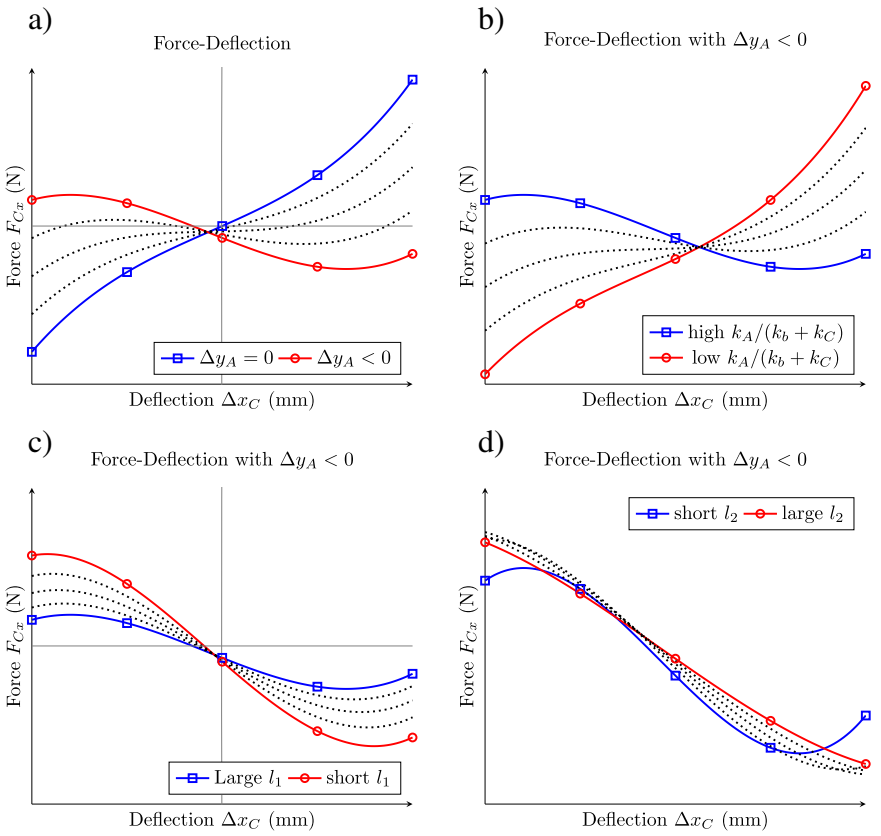

Fig. 3. Stiffness behavior of the slider at point *C* with respect the design parameters. (a) Changes in Δy_A. (b) Changes in joints' torsion stiffness. (c) Shortening of link *l* while keeping links perpendicular. (d) Enlargement of link l_2.

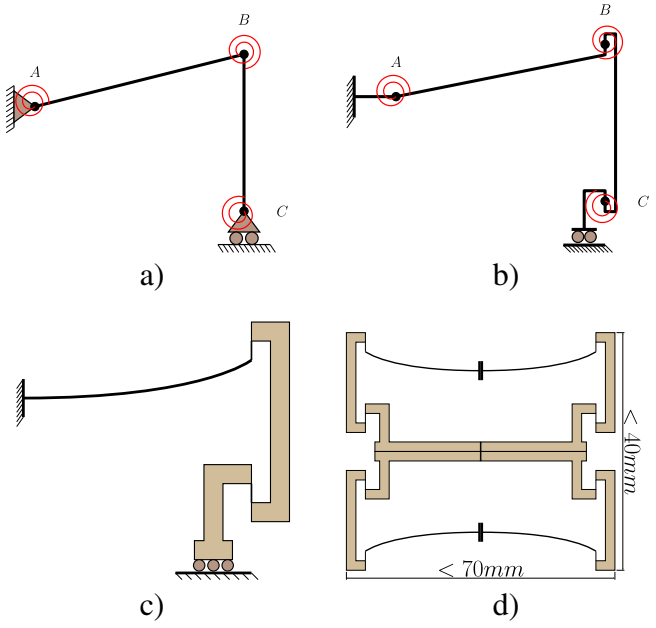

Fig. 4. Conceptual design of the balancer. (a) The rigid-body linkage. (b) The PRB model. (c) The compliant mechanism. (d) The compliant mechanism mirrored in two axes.

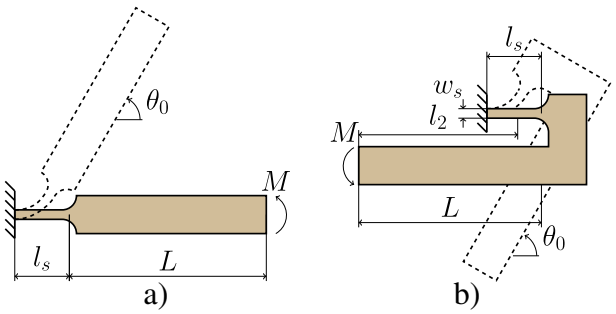

Fig. 5. Pseudo-rigid-body model for lumped compliance of the smallest flexure. (a) Cantilever beam as assumed by conventional model. (b) Inverted cantilever beam as assumed for link l_2 with either joints B or C.

3.1. Conceptual design

The balancer is constrained to fit in a ∅40 mm × 30 mm cylinder—dimensions of an acceptable surgical handcraft tool [3]. The PRB model of the linkage is shown in Fig. 4b.

Since the torsion stiffness at hinges B and C should be low, it is opted for flexures with lumped compliance with the added advantage of well defined hinge locations. On the downside slender flexures with lumped compliance cannot withstand compressive loads due to buckling effects. Fig. 4c shows the conceptual design for the fully compliant rocker–slider linkage in which the flexures are loaded under tensile force.

To construct a fully compliant prismatic pair, and avoid the use of complex compliant suspensions, the geometry is mirrored twice, first with respect to a horizontal axis at the sliding ground, and then with respect to a vertical axis through the ground point, see Fig. 4d.

3.2. Balancer dimensioning

The prototype mechanism is made out of titanium grade 5 with a Young's modulus of $E = 113.9\text{kN/mm}^2$ and an allowable strength limit of $\sigma_a = 500\text{N/mm}^2$ equal to the fatigue strength limit (55% of the tensile strength).

The dimensioning of link l_2 and joints B and C as flexures is performed by the use of a modified version of the PRB model for lumped compliance as shown in Fig. 5. Here it is assumed that link l_2 together with either joint B or C forms the cantilever beam on which the PRB model is applied.

The dimensioning of the preloading beam which is formed by link l_1 and joint A is done by setting a length/width ratio which avoids axial overloading of flexures B and C due to the application of preloading deflection Δy_A. Once the length/width ratio is set and the dimensions of the preloading beam are known, the dimensions of link l_1 and stiffness of joint A are determined by use of the PRB model for distributed compliance. The preloading beam has a rectangular constant cross section area.

3.2.1. lumped compliance flexure — joints B and C

The prototype manufacturing is done by wire EDM which imposes a minimum in-plane width of $w_s = 0.2\text{mm}$ for the smallest flexure. The out-of-plane thickness is set to $t = 6\text{mm}$ to avoid out-of-plane deflections, such value provides a stiffness ratio of $t^2/w_s^2 = 900$ between lateral deflections at the smallest flexure. The length of the smallest flexure is set to $l_s = 2\text{mm}$, this is a length/in-plane-width ratio of 10. Assuming that the flexure undergoes bending under pure moment, such a ratio in combination with

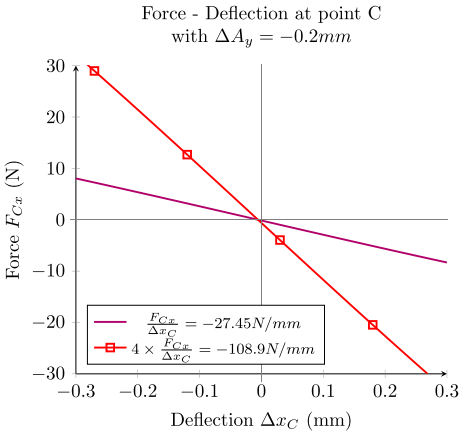

Fig. 6. Force-deflection behavior of the slider–rocker linkage with torsion springs. The model when preloaded exhibits negative stiffness.

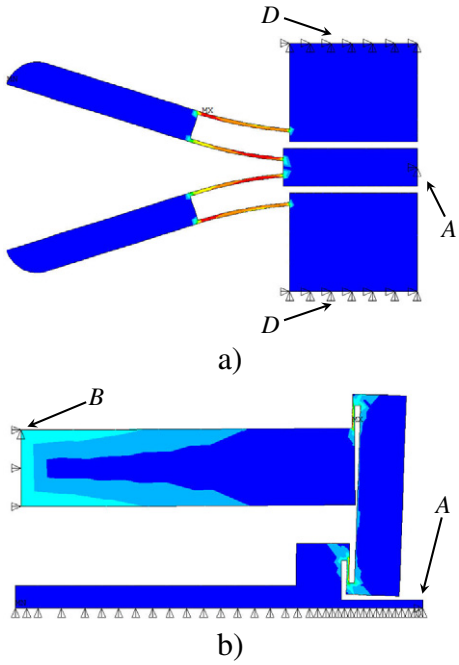

Fig. 7. Stress distribution as result of FEA. Points A and B are the actuation and pre-loading ports, respectively. Point D is the ground port. (a) The grasper exhibits the maximum stress at its full open configuration. (b) The balancer exhibits its maximum stress at full shuttle displacement while the pre-loading displacement is kept.

Bernoulli–Euler and bending stress equations guarantees a maximum admissible deflection of $\theta_s = 0.088\text{rad}$ below the allowable strength limit, see Eq.(7).

$$\frac{l_s}{w_s} = \frac{E\theta_s}{2\sigma_a} \tag{7}$$

For the latter dimensions the PRB model for lumped compliance predicts a torsional stiffness of the smallest flexures as,

$$k_s = \frac{EI_s}{l_s} = 227.8\text{Nmm/rad}. \tag{8}$$

According to the PRB model for lumped compliance the length of link l_2 should be at least 10 times the length of the smallest flexure l_s. But such value would violate the constraint of the balancer to fit in cylinder of ∅40 mm, see the conceptual design in Fig. 4d. The value of link 2 is then set to $l_2 = 13.75\text{mm}$.

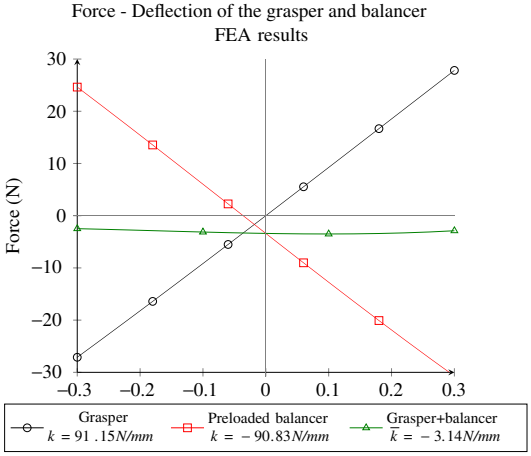

Fig. 8. Force-deflection behavior predicted by finite elements analysis of the grasper, the preloaded balancer and combined grasper and preloaded balancer.

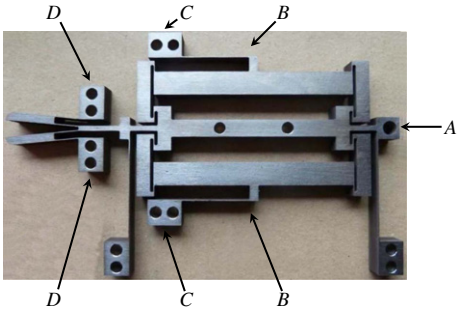

Fig. 9. Titanium prototype of the fully compliant grasper. Points A and B are the actuation and pre-loading ports, respectively. Points C and D are he ground ports.

Given the dimensions of the cross section, the limit for the axial load on the smallest flexure is $f_s = 400\text{N}$. This value results by taking a safety factor of 1.5 over the allowable strength limit σ_a.

3.2.2. distributed compliance flexure — joint A

The force that the preloading beam – the one replacing link l_1 – can exert over the smallest flexure is limited to the value f_s. To prevent failure of the smallest flexure by the pre-loading beam, a length/width ratio is set. For small deflections the transverse force of the preloading beam is

$$f_s = \frac{3EI_p\Delta y_A}{l_p^3} \tag{9}$$

where l_p is the length of the beam and I_p is the area moment of inertia. Replacing I_p for the expression of a constant rectangular cross-section, assuming a pre-loading deflection $\Delta y_A = 0.2\text{mm}$, and by setting f_s as a limit, yields

$$\frac{l_p}{w_p} > \sqrt[3]{\frac{E\Delta y_A t}{4f_s}} = 4.4. \tag{10}$$

The length of pre-loading beam is set to $l_p = 29.5\text{mm}$, such value is below 30mm which is a limit imposed by the symmetry of the balancer and the constraint to fit in a cylinder of 70mm length. With the length of the pre-loading beam, its in-plane width is set at the limit of the 4.4 ratio as $w_p = 6.7\text{mm}$.

For the given dimension of the pre-loading beam, the PRB model for distributed compliance using a $\gamma = 0.852$ and $K_\Theta = 2.65$ predicts the torsion stiffness and the link length as

$$k_p = \frac{\gamma K_\Theta EI_p}{l_p} = 1309900\text{Nmm/rad} \tag{11}$$

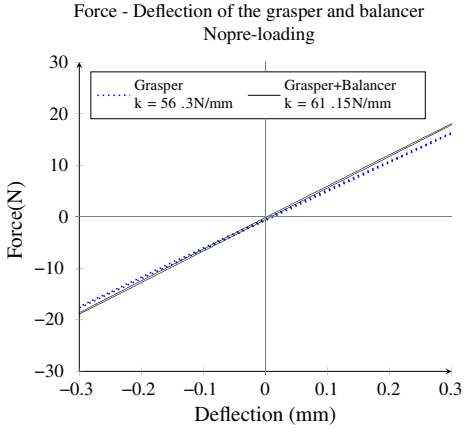

Fig. 10. Force-deflection behavior of titanium prototype for load-cases 1 and 2.

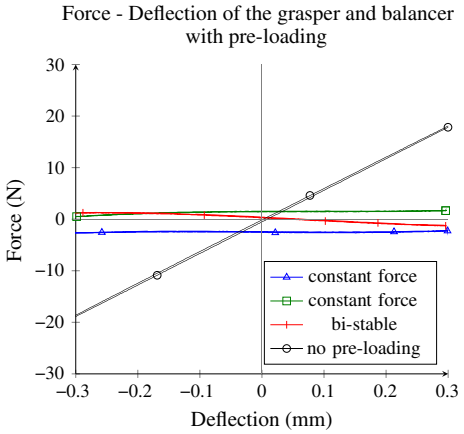

Fig. 11. Force-deflection behavior of titanium prototype for the grasper and balancer with different pre-loading values (load-case 3).

$$l_1 = \gamma l_p = 25.134\text{mm}. \tag{12}$$

Replacing the values of the design parameters in the slider–rocker linkage model, a negative stiffness of $\frac{F_{Cx}}{\Delta x_C} = -27.45\text{N/mm}$ is predicted when a pre-load of $\Delta y_A = 0.2\text{mm}$ is applied. The linkage model predicts as well a positive stiffness of $\frac{F_{Cx}}{\Delta x_C} = 2.71\text{N/mm}$ when no pre-load is present. The force-displacement behavior for negative and positive stiffness exhibits a linear correlation of $r^2 = 1$ and $r^2 = 0.997$, respectively, for the range of motion $\Delta x_C = [-0.3\text{mm}; 0.3\text{mm}]$. This means that in theory the fully compliant balancer which is a composition of four slider–rocker linkages (see Fig. 4d) should be able to exert a linear negative stiffness of − 109.8N/mm over the compliant grasper.

4. Analysis

Virtual validation of the grasper and balancer design is done through the use of non-linear finite elements using 2D quadratic triangular elements for plane stress with large deflections and small strain. Beam elements are not used since it is desired to observe the strain energy distribution and stress concentration across the material.

The balancer analysis is performed by displacement control in three time steps. The first time step pre-loads the balancer at port *B*. The second and third time steps correspond to a forward and backward displacement applied at the actuation port *A* of the slider. Boundary conditions are applied to restrict the vertical displacement of the shuttle and the horizontal displacement of the pre-loading beam (Fig. 6).

The grasper analysis is performed by displacement control in two time steps, corresponding to opening and closing of the grasper (displacement at port A). Motion is constrained in all the degrees of freedom at the grasper's ground port D.

Results of the stress distribution, port numbering and boundary condition setting for the balancer and grasper are shown in Fig. 7.

The analysis indicates that for a maximum deflection of 0.3mm from equilibrium, the maximum equivalent stress for the preloaded balancer is about 555N/mm^2 exhibiting a negative stiffness of − 90.83N/mm with − 0.9998 correlation. The maximum equivalent stress for the grasper is about 531N/mm^2 exhibiting a positive stiffness of 91.15 with 0.9999 correlation. The mean stiffness value for the combined balancer and grasper is about − 3.14N/mm with a standard deviation of 0.3112, see Fig. 8. The latter values correspond with a predicted actuation energy reduction of about 83.64 % between the unbalanced and balanced grasper.

The analysis indicates as well that considering the smallest flexures to be under pure bending load is not wrong. The stress distribution along the flexures is uniform which indicates that the moment acting along the flexure is almost constant. A mesh dependency study shows a variation of the maximum stress at the smallest flexures of about 5.4% for a mesh refinement with a factor of 10.

Table 1
Load-case 3 — measurement results.

Case	Constant positive force	Constant negative force	Bistable
Standard deviation (N)	0.4648	0.1670	0.4217
Mean value (N)	1.1691	−2.5674	0.9054
Hysteresis (mJ)	0.0492	0.0752	0.0653
Strain energy reduction	86.24%	80.84%	91.75%

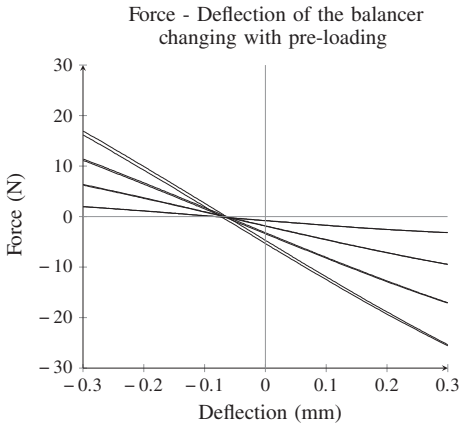

Fig. 12. Force-deflection behavior of titanium prototype for the balancer. Different pre-loading values ranging from [0 mm-0.24 mm] inducing negative stiffness (load-case 4).

5. Results

Experimental validation of the design is done through manufacturing of a titanium prototype in which force-deflection measurements are performed. The displacement range is prescribed at point *A*, see Fig. 9. while force **F** is measured at the same time. Four load cases are measured.

Load-case 1 Force deflection of the grasper. *D* points are fixed, *C* points are free. No preload applied at *B* points.
Load-case 2 Force deflection of the grasper and balancer. *C* and *D* points are fixed. No preload applied at *B* points.
Load-case 3 Force deflection of the grasper and balancer with preload. *C* and *D* points are fixed. At *B* points a preload displacement of about 0.3mm is applied. Preload is applied through an adjustment screw M4 × 0.5 which transmits motion to a lever with a geometrical advantage of 1 in 5. Such arrangement allows incrementing preloading with an accuracy of about 0.025 mm per each quarter turn of the screw.
Load-case 4 Force deflection of the balancer. *C* points are fixed, *D* points are free, preload is applied at *B*.

Fig. 10 shows the measurement results for load-cases 1 and 2. The measurements indicate that the grasper stiffness is about $k = 56.33\text{N/mm}$, while the stiffness of the combined grasper and balancer is about $k = 61.15\text{N/mm}$ with a hysteresis of about 0.1019mJ. This means that the stiffness of the balancer is about $k = 4.82\text{N/mm}$. Such value presents a deviation of 55.5% with respect to the predicted value of $k = 10.84\text{N/mm}$ ($2.71\text{N/mm} \times 4$) by the PRB model. Such deviation is attributed to several facts, (i) the preloading beam exhibits a length-width ratio 4.4 which combined with out-of-plane thickness creates a proportion in which the shear effects are high enough to be considered and are not accounted by the PRB model, hence the behavior of the beam is not accurately predicted, (ii) the condition of a ratio of 1:10 between the flexure and the rigid portion of link was not respected, which deviates the kinematic predictions of the PRB model, (iii) the stiffness from the fixation flexure CB was not considered during modeling, (iv) the in-plane and out-of-plane torsional preloading due to the clamping bolts at points C and D was not considered, and (v) when the preloading deflection is applied at point B the clamping beam BC undergoes lateral stiffening effects which reduces the ability of the balancer to induce negative stiffness. The influence of such stiffening effects has not been studied.

Fig. 11 shows the measurement results for load-cases 2 and 3. Measurement results from load-case 3 are summarized in Table 1. The compliant mechanism when preloaded exhibits a behavior of either bistability, constant positive force or constant negative force. Strain energies are computed by numerical integration of the areas beneath the force-deflection functions. Hysteresis is computed as the difference in strain energy during three cycles of loading and unloading of one single actuation measurement, while the strain energy reduction is computed as the difference in strain energy during actuation of the system with and without preloading.

Bistability is obtained when the system is over preloaded. Points C and D are initially fixed, and then preload displacement Δy_A is increased until bistability occurs. Such behavior was exhibited for a preload displacement of about $\Delta y_A = 0.3 \pm 0.025\text{mm}$.

Constant positive force or constant negative force is associated to a lateral shifting of the equilibrium point on either the balancer or the grasper. Lateral shifting of the equilibrium point does not depend on the preloading displacement Δy_A at *B* points as shown by the measurements of load-case 4. Fig. 12 shows that the equilibrium point is not sensitive to the pre-load deflection at *B* points. Preloading is not a sufficient condition for equilibrium shifting for this particular design. The latter comes as a result of the two-axis symmetry of the rocker–slider linkage. The lateral shifting of the equilibrium point on the grasper and balancer is associated to the initial stresses induced by the clamping bolts used to fix points *C* and *D*. These initial stresses cause a lateral shifting of the equilibrium point between the balancer and the grasper. The sensitivity of the system to the offset caused by the clamping bolts has not been investigated.

The results of the balanced compliant grasper with respect to its unbalanced state, can be seen in Table. 1 as the strain energy reduction percentage. Table 2 shows the stiffness values predicted by the PRB model and FE analysis next to the stiffness from the prototype measurements.

Table 2
Consolidated stiffness values from measurement and models.

Model	Balancer stiffness		Grasper stiffness
	No preload	With preload	
	(N/mm)	(N/mm)	(N/mm)
PRB model	10.84	−109.8	–
FE analysis	9.95	−90.83	91.15
Prototype measurements	4.82	−58.99	56.33

6. Conclusions

In this work it has been shown the rigid-body-replacement method is a feasible method for the design of statically balanced compliant mechanisms. The procedure for the replacement of the kinematic pairs by flexures proved the pseudo-rigid-body model as a practical tool in the design of statically balanced compliant mechanisms. Even with the limitations of the PRB model to account for shearing effects and combined load conditions, the model led to a design which proves the concept viability by the use of simple hand calculations.

The design can be refined by the use of size optimization in order to improve the behavior of the design.

It is important to mention that clamping a tunable statically balanced compliant mechanism into a frame is an important issue that must be considered at the conceptual design stage, since clamping could lead to prestressing effects which can cause shifting of the equilibrium point and stiffness deviations which lead to undesired behaviors.

A sensitivity analysis must be conducted to verify the effects of shearing and their influence in the deviations observed between models.

Acknowledgement

This research is part of the “VIDI” Innovational Research Incentives Scheme grant for the project “Statically Balanced Compliant Mechanisms”, NWO-STW 7583.

References

[1] J.L. Herder, M.J. Horward, W. Sjoerdsma, A laparoscopic grasper with force perception, Minim. Invasive Ther. Allied Technol. 6 (4) (1997) 279–286.
[2] J.L. Herder, F.P. van den Berg, Statically balanced compliant mechanisms (SBCM's), an example and prospects, Proceedings of the ASME Design Engineering Technical Conference, ASME, 2000.
[3] A. Stapel, J.L. Herder, Feasibility study of a fully compliant statically balanced laparoscopy grasper, Proceedings of the ASME Design Engineering Technical Conference, Vol. 2, ASME 2004, pp. 635–643.
[4] D.J.B.A. de Lange, M. Langelaar, J.L. Herder, Design of a statically balanced compliant laparoscopic grasper using topology optimization, Proceedings of the ASME Design Engineering Technical Conference, Vol. 2, ASME 2008, pp. 293–305.
[5] N. Tolou, J.L. Herder, Concept and Modeling of a Statically Balanced Compliant Laparoscopic Grasper, Proceedings of the ASME Design Engineering Technical Conference, Vol. 7 2009, pp. 163–170.
[6] K. Hoetmer, G. Woo, C. Kim, J.L. Herder, Negative stiffness building blocks for statically balanced compliant mechanisms: design and testing, J. Mech. Robot. 2 (4) (2010) 041007-7.
[7] G.K. Ananthasuresh, S. Kota, N. Kikuchi, Strategies for systematic synthesis of compliant MEMS, American Society of Mechanical Engineers, Dynamic Systems and Control Division DSC, Vol. 55-2 of Proceedings of the 1994 International Mechanical Engineering Congress and Exposition, ASME, Chicago, IL, USA 1994, pp. 677–686.
[8] G.K. Ananthasuresh, Optimal Synthesis Methods for MEMS, Kluwer Academic, Boston, 2003.
[9] C.J. Kim, S. Kota, Y.-M. Moon, An instant center approach toward the conceptual design of compliant mechanisms, J. Mech. Des. 128 (3) (2006) 542–550.
[10] C.J. Kim, Y.M. Moon, S. Kota, A building block approach to the conceptual synthesis of compliant mechanisms utilizing compliance and stiffness ellipsoids, Journal of Mechanical Design 130 (2) (2008) 022308.
[11] M.D. Berglund, S.P. Magleby, L.L. Howell, Design rules for selecting and designing compliant mechanisms for rigid-body replacement synthesis, Proceedings of the ASME Design Engineering Technical Conference, ASME, Baltimore, Maryland, USA, 2000.
[12] L.L. Howell, A. Midha, A method for the design of compliant mechanisms with small-length flexural pivots, J. Mech. Des. 116 (1) (1994) 280–290.
[13] L.L. Howell, Compliant Mechanisms, John Wley & Sons, Inc., New York, 2001.
[14] J.A. Gallego Sánchez, Statically Balanced Compliant Mechanisms: Theory and Synthesis, PhD Thesis, Delft University of Technology, Delft, The Netherlands, 2013.